Influence of the scattered Cherenkov light on the width of shower images as measured in the EAS fluorescence experiments

M. Giller, G. Wieczorek

Accepted Manuscript

Influence of the scattered Cherenkov light on the width of shower images as measured in the EAS fluorescence experiments

M. Giller, G. Wieczorek

Please cite this article as: M. Giller, G. Wieczorek, Influence of the scattered Cherenkov light on the width of shower images as measured in the EAS fluorescence experiments, *Astroparticle Physics* (2009), doi: 10.1016/j.astropartphys.2009.01.003

Influence of the scattered Cherenkov light on the width of shower images as measured in the EAS fluorescence experiments
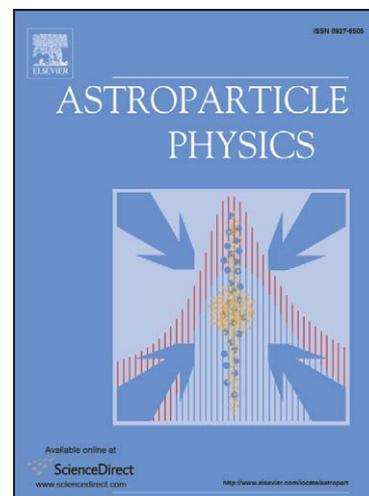
M. Giller [*] and G. Wieczorek

Department of Experimental Physics, University of Lodz, Pomorska 149/153, 90-236, Lodz, Poland

Abstract

We calculate the lateral distribution of Cherenkov light at different levels of shower development. The calculations use the universal characteristics of large showers. We derive that the angular and lateral distributions of Cherenkov photons emitted by a shower path element depend only on the shower age and height in the atmosphere of this element. The width of a shower image in the Cherenkov scattered light also depends, however, on the zenith angle and X_{max}. We also show that below shower maximum it is considerably wider than the width in the fluorescence light.

Key words: Ultra-high energy cosmic rays, extensive air showers, fluorescence method of shower detection
PACS: 96.50.sd

1 Introduction

Extensive Air Showers (EAS) produced in the atmosphere by cosmic ray particles cause excitation of its atoms and a subsequent isotropic emission of fluorescence light by nitrogen molecules. If the energies of cosmic particles are large enough (above $\sim 10^{17}$ eV) this light can be detected by earth-based telescopes, so that the showers can be seen from the side from tens of kilometers away.

Another big advantage of the fluorescence technique is the possibility of registering a light image of a shower from which the shower curve – the number

---

[*] email: maria.giller@kfd2.phys.uni.lodz.pl

of particles or, strictly speaking, the energy deposit as a function of depth in the atmosphere – can be deduced. This is so because experiments show that the fluorescence light emitted by a shower path element is proportional to the energy loss of shower particles along this element [1,2].

Having determined a shower curve one can calculate the energy of the primary particle (by simply integrating the energy deposit along the track in the atmosphere) in a way (practically) independent of its mass and the actual (unknown) high energy interaction characteristics [3].

The fluorescence technique was used with success by the Fly's Eye experiment [4] and by its successors, the various set-ups of HiRes (see e.g. [5,6]).

In the recently built Pierre Auger Observatory – Southern Site in Argentina [7] this technique has also been applied, but here, apart from the optical telescopes, there are 1600 shower particle detectors covering 3000 km^2. As the fluorescence detectors operate on clear nights only, in contrast with the particle detectors which are active all the time, the energies of showers registered by the latter (obtained by another method) can be calibrated by the sample of showers registered by both types of detectors.

The problem is that some fraction of shower particles (~ 0.36 [8]) also emit Cherenkov light (ChL). Its direction is almost the same as that of the emitting particle velocity, so one might think that this light will not add to the fluorescence flux detected by a telescope situated at a large distance (more than a few km) from the shower. However, the number of Ch photons produced by a high energy particle is $5 – 6$ larger than its fluorescence (FL) photon count. Thus, many Ch photons accumulate as the shower develops and those scattered sideways constitute a non-negligible fraction of the total light registred by a telescope. If not properly substracted, they might mimic a larger number of electrons (and larger energy deposit) in the shower.

This effect has been first aknowledged and allowed for by the Fly's Eye Collaboration [4]. Later some other methods to take it into account have been proposed [9–11]. In these papers, however, it was only the total number of Ch photons emitted from consecutive shower track elements that were taken into consideration. Here we are concerned with their lateral distributions (with respect to the shower axis).

A shower image (e.g. as measured in the Auger experiment) is registered typically by a line of hit photomultipliers on a telescope camera. The closer the shower the broader the image line, because shower particles (mainly electrons of both charges) have some lateral spread, due to the Coulomb scattering in the atmosphere. The breadth of the shower image in both ChL and FL has not been investigated – although, as we shall show in this paper, an answer to this question is important. Góra et al [12] proposed that it is the FL that

2

determines the lateral width of the shower image. In this paper we shall show that it is true only for upper parts of a shower (above its maximum). Widths of images below shower maxima are strongly affected by Ch scattered light.

Thus, to correctly determine the energy deposit at a given level in the atmosphere (proportional to the FL emitted there), it is necessary to know exactly how ChL is distributed over the light image, not only along but also across the shower. Only then will one be able to subtract it properly. This is what we shall deal with in this paper (for some preliminary results, see [13]).

It is clear that the lateral distribution of ChL (LDCh) *observed* at a given level of shower development depends on the angular and lateral distributions of electrons emitting ChL (we shall call them "Ch electrons") at all higher levels. We shall show that the above distributions of ChL *produced* at some level of the shower development depend *only* on the shower age and the height of this level. We shall derive how this follows from the uniquenes of various electron distributions in all large showers (the similarity of showers).

2 The method of calculation of the lateral distribution of ChL (LDCh)

We show here that due to the similarity of high energy showers [8,9,14] it is possible to calculate the lateral distribution of ChL (LDCh) without time-consuming shower simulations, but in an analytical way (with numerical calculations of integrals), using the various earlier determined electron distributions which are universal.

2.1 The general idea

The similarity of different showers is based on comparing their characteristics at levels with the same age parameter s.

The age of a particle cascade (at a given level of its development) was introduced while analytically describing developments of *pure electromagnetic* cascades (initiated by primary electron or photon). It was defined as

$$s = \frac{3t}{t + 2\ln(E_0/\varepsilon)} \tag{1}$$

where t is the depth in cascade units, E_0 is the particle initial energy and ε is the critical energy of the medium. The spectra of high energy electrons (with

3

energies $E \gg \varepsilon$) were shown to be proportional to $E^{-(s+1)}dE$ [15,16].

Formula (1) was first applied by Hillas [17] to cosmic ray showers, initiated by *hadrons*, in the form

$$s = \frac{3X}{(X + 2X_{max})} \tag{2}$$

where the term $\ln(E_0/\varepsilon)$, being the depth of the cascade maximum, has been replaced by X_{max} – the depth of the shower maximum. He also proposed a form of the energy distribution of electrons depending on s.

Following his idea we have analysed in the earlier papers of our group various electron distributions in showers simulated with the CORSIKA code [18]. We have come to the conclusion that high energy showers are similar to each other in the following sense:

– the shape of the electron energy spectrum at a given level in the atmosphere depends only on the stage of the shower development there, i.e. on the age parameter s [8]; it does not depend on primary particle mass or energy (the same conclusion was obtained by Nerling et al [10]),
– the angular distribution of electrons with a fixed energy depends on this energy only – it is the same anywhere in the shower [9]; from the two statements above it follows that the angular distribution of all electrons (with any energy) depends on the shower age only,
– the lateral distribution of electrons, if distances are expressed in the Molière unit r_M at the level in consideration, depends on the shower age only [14] (the same holds for electrons with a fixed energy [19]).

It has also been established that fluctuations of the above distributions from shower to shower are very small, so that these distributions can be parametrised and used to describe any individual shower. In particular, when observing a shower with a fluorescence detector and determining the position of the shower maximum, it is possible to asign age parameters to various depths along the shower track. Then the distributions of energy, angle and lateral distance of electrons, at various positions along the shower, can be predicted.

It should be noted, however, that determining shower age from X_{max} only i.e. independently of the depth of the first interaction, X_1, makes sense if $X_1 \ll X_{max}$. For the highest energy showers, when $\overline{X_1} \simeq 50$ g cm^{-2} for protons (and even smaller for heavier primaries) and $X_{max} > 700$ g cm^{-2}, this condition is fulfilled. It means that in this case the *actual* stage of shower development is well determinied by formula (2). It is obvious that for a neutrino initiated shower the depth X in formula (2) must be measured from the first interaction rather than from the top of the atmosphere.

4

As we are concerned here with the Cherenkov light, emitted only by electrons with energies above some threshold energy (dependent on the atmospheric density and, therefore, on the height h in the atmosphere), the Cherenkov characteristics at a given level depend not only on the age parameter but on the height as well. However, since we have already found the angular and lateral distributions of electrons with a given energy, we can easily calculate these distributions for all electrons emitting Ch light, by integrating the former above the threshold energy $E_{th}(h)$.

It is convenient to assign to any electron a weight $Y_{ch}(E/E_{th})$, proportional to the number of Ch photons it emits per unit path (in g cm^{-2}). This weight equals

$$Y_{ch}\left(\frac{E}{E_{th}}\right) = 1 - \left(\frac{E_{th}}{E}\right)^2 \tag{3}$$

Adding up all these numbers at a given level gives what we shall call the number of Cherenkov (Ch) electrons. Multiplying this number by the amount of Ch light produced by an electron with $E \gg E_{th}$ per unit path, in g cm^{-2} (a known constant), gives the total Ch light produced at a given level per 1 g cm^{-2} of shower track.

2.2 Calculations

The LDCh at a given depth of shower development s_{obs}, being at height h_{obs}, is a sum (integral) of lateral distributions of ChL resulting from Ch emission at all levels above the given one. It depends on the angular, $G_\theta^e(\theta; s < s_{obs}, h > h_{obs})$, and lateral, $G_x^e(x; s < s_{obs}, h > h_{obs})$, distributions of Ch electrons in the shower above this level. Here $x = r/r_M$. As we have just discussed these distributions of Ch electrons depend on the age s of the considered level and its height h (strictly speaking – on the air density).

2.2.1 Angular distribution of Ch electrons, $G_\theta^e(\theta; s, h)$

The angular distribution $G_\theta^e(\theta; s, h)$ (per unit angle θ) can be calculated from the known angular distributions of electrons with fixed energies, $g_\theta(\theta; E)$ (per unit solid angle) [9], and the energy spectrum of all electrons at level s, $f(E; s)$ [8,10],

$$G_\theta^e(\theta; s, h) = \frac{2\pi \sin\theta}{F(s, h)} \int\limits_{E_{th}(h)}^{\infty} g_\theta(\theta; E) \cdot f(E; s) \cdot Y_{Ch}\left(\frac{E}{E_{th}}\right) \cdot dE \tag{4}$$

5

where $F(s, h)$ equals

$$F(s, h) = \int\limits_{E_{th}(h)}^{\infty} f(E, s)\, Y_{Ch}\left(\frac{E}{E_{th}}\right)\, dE \tag{5}$$

The normalisation of $G_\theta^e(\theta; s, h)$ is such that

$$\int G_\theta^e(\theta; s, h)\, d\theta = 1 \tag{6}$$

$F(s, h)$ is the ratio of the number of Ch electrons to the total number of electrons at this level. It has been calculated in [8] that this number does not change much along the shower, being equal ~ 0.36. This is a result of two competing effects: the deeper along the shower, the steeper becomes the electron energy spectrum, but at the same time the threshold for Ch emission diminishes. Once the electron energy spectra $f(E; s)$ are known, $F(s, h)$ can be calculated and parametrized as a function of s and h [8].

Both $f(E; s)$ and $g_\theta(\theta; E)$ in (4) have been obtained from a sample of simulated showers with $E = 10^{19}$ eV and 10^{20} eV, initiated by a primary proton or iron nucleus. Thanks to a large number of shower particles in such showers, the above distributions fluctuate very little from shower to shower so that the samples of simulated showers did not have to be large (it was ~ 20 showers for each combination of E and mass).

The electron angular distributions, $G_\theta^e(\theta; s, h)$, have been calculated as histograms for different s and h.

2.2.2 Angular distribution of Cherenkov light (ChL), $G_\theta^{Ch}(\theta; s, h)$, emitted at level (s, h)

Having the angular distributions of electrons we can easily allow for the ChL angle of emission and calculate the angular distribution of the ChL emitted at a given level, $G_\theta^{Ch}(\theta; s, h)$. This is a very small effect since the Cherenkov angle is less than $1.2°$ – the emission angle at sea level by an electron with energy $E \gg E_{th} = 21$ MeV.

The idea of calculating $G_\theta^{Ch}(\theta; s, h)$ is shown in Fig. 1. The radii of rings are proportional to the bins of electron angle θ. The number of electrons with angles within a given bin $\Delta\theta$ equals $G_\theta^e(\theta; s, h)\Delta\theta$. Each electron emits ChL at an angle θ_{Ch} (the small ring around an electron direction). The fraction of Ch photons falling into a particular ring $(\theta, \theta + \Delta\theta)$ equals the fraction of the Ch ring circumference within that ring (the dark parts of the Ch ring). Thus,
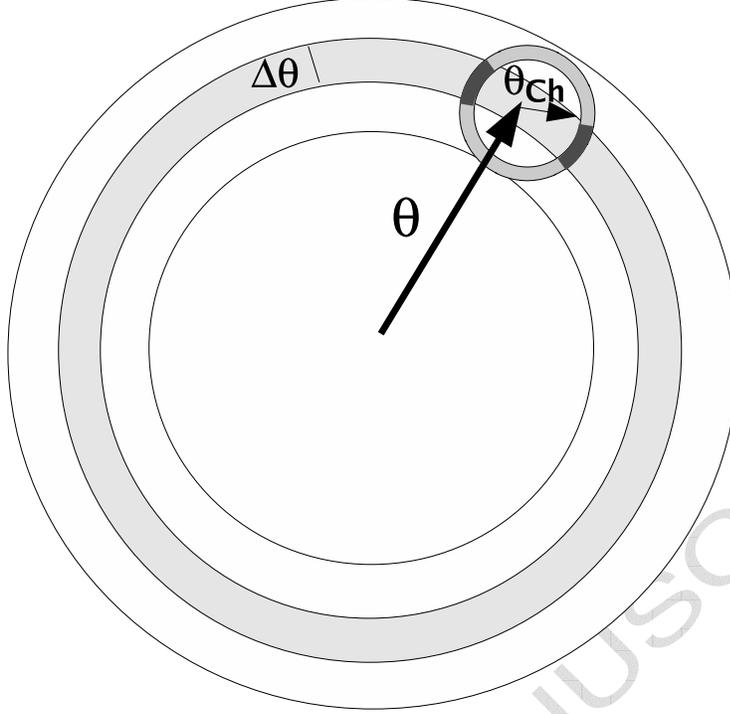
6

Fig. 1. Illustration of the method of taking into account the Cherenkov cone: the angular distribution of Ch electrons gives the number of electrons within each annular ring $(\theta, \theta + \Delta\theta)$. Ch light is emitted at an angle θ_{ch} to the electron direction. The number of produced Ch photons, having angles to the shower axis within this ring, is proportional to the fraction of the circumference $(2\pi\theta_{ch})$ lying inside this ring (the dark shaded regions).

the angular distribution of ChL equals

$$G_\theta^{Ch}(\theta_i; s, h)\Delta\theta_i = A \sum_j G_\theta^e(\theta_j; s, h) \cdot u_{ji}\Delta\theta_j \tag{7}$$

where u_{ji} is the fraction of ChL emitted by an electron with angle θ_j, falling into the ring $(\theta_i, \theta + \Delta\theta_i)$ (found from simple geometric considerations); A is the normalization constant.

The results of our calculations are presented in Fig. 2 for several values of s and h. We have also shown the curves obtained by Nerling et al [10] who parametrised the results of Monte-Carlo shower simulations with CORSIKA. The agreement is very good apart from the angles $\gtrsim 1$ rad. Nevertheless, the differences are in a region where the emitted flux is more than three orders of magnitude less than that at smaller angles. What we are finally aiming at is to calculate the *scattered* ChL, to which the contribution of this direct light is very small at large angles.
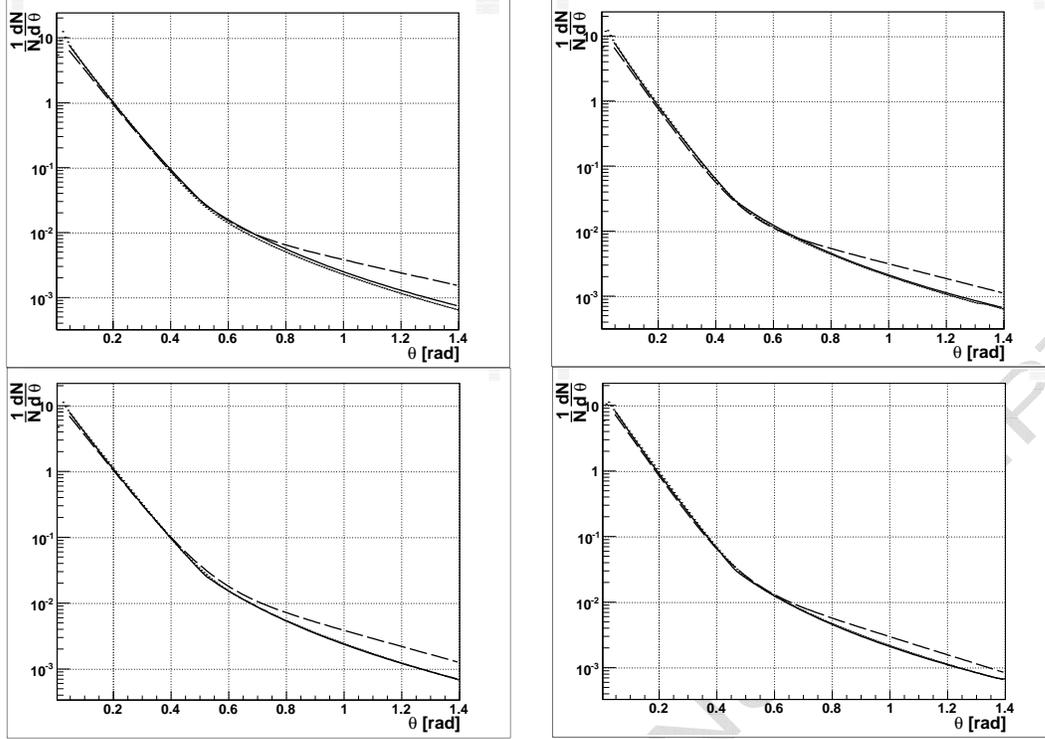
7

Fig. 2. Angular distributions of Ch light, $G_\theta^{Ch}(\theta; s, h)$, emitted at $s=1$ – two upper graphs and $s=1.2$, – lower graphs, left graphs – $h=5$ km, right graphs – $h=8$ km. The analytical parametrizations are practically indiscernible from the numerical results. Also shown are simulation results of Nerling et al [10], which are slightly higher at large angles (dashed lines).

2.2.3 Lateral distribution (LD) of Ch electrons, $G_r^e(r; s, h)$, at level (s, h)

In an earlier paper of our group [14] it was shown that LD of all electrons at a given level in the shower depended on the shower age only if the distance to the shower core was expressed in the Molière unit at this level. When one is interested in the Ch electrons only, then it is natural to examine LD(E), i.e. LD of electrons with fixed energies E, and then integrate them above the corresponding threshold energy at the level's height.

An analysis of the lateral distributions of electrons with fixed energies was done by Giller et al [19]. It was shown that if electrons with a fixed energy (in practice, from a narrow energy band) were considered, their LD depended only on the shower age s at the corresponding level.

A new distance unit was used there, r_E, depending on the electron energy E and equal to

$$r_E = X_0 \cdot 21 \text{ MeV}/E \tag{8}$$

8

where $X_0 = 37$ g cm^{-2} is the air cascade unit. Our distance unit r_E differs from the Molière radius in substituting the electron energy E for the critical energy of the medium ($\sim$80 MeV for air). By doing so the parameters describing LD(E) for different energies do not vary much and are more easily described in an analytical way.

One may wonder why LD(E), for any particular electron energy E, depends on shower age s, while the angular distribution does not. It is because the air density in the atmosphere is not uniform; in particular, it has smaller density higher up. The inhomogeneity of the medium does not affect the angular distributions. For an electron with a given energy the angles of its more energetic parents do not play any significant role, as the scattering angles add in quadrature.

The same would be for distances in a uniform medium. However, in the real atmosphere the lateral distances of the parents, as it turns out, are not negligible in comparison with those of their lower energy doughters, because of lower densities higher up.

To see whether the LD of all Ch electrons are important in calculating the LDCh (LD of Ch light) we first calculated the mean squares of LD(E), $\langle r^2(s; E) \rangle$.

LD(E) are very well described by Nishimura-Kamata-like functions of the form

$$g_r(r; s, E) = \frac{1}{N_e} \cdot \frac{dN_e}{d\log(x)} = Cx^\alpha(1 + kx)^{-\beta} \tag{9}$$

where $x = r/r_E$ and the parameters α, β and k depend on E, and k depends also on s [19]. Thus, $\langle x^2(s; E) \rangle$ can be found analytically and the result is

$$\left\langle x^2(s; E) \right\rangle = k^{-2} \frac{\Gamma(\alpha + 2)\,\Gamma(\beta - (\alpha + 2))}{\Gamma(\alpha)\,\Gamma(\beta - \alpha)} \tag{10}$$

and

$$\left\langle r^2(s; E) \right\rangle = \left\langle x^2(s, E) \right\rangle \cdot r_E^2 \tag{11}$$

To calculate $\langle r^2(s, h) \rangle$ of all Ch electrons at a given level (s,h) one simply needs to integrate the above mean squares over electron energies, weighted with their energy distribution $f(E; s)$ and the Ch yield $Y_{ch}\left(\frac{E}{E_{th}}\right)$ (formula 3):

$$r_\perp \equiv \sqrt{\langle r^2(s, h) \rangle} = \sqrt{\frac{\int_{E_{th}(h)}^\infty \left\langle r^2(E; s, h) \right\rangle \cdot f(E; s) \cdot Y_{Ch}\left(\frac{E}{E_{th}}\right) \cdot dE}{\int_{E_{th}(h)}^\infty f(E; s) \cdot Y_{Ch}\left(\frac{E}{E_{th}}\right) \cdot dE}} \tag{12}$$

9

The LD of Ch electrons at level (s, h) equals

$$G_r^e(r; s, h) = \frac{1}{F(s, h)} \int_{E_{th}}^{E_0} g_r(r; s, h) f(E; s) Y_{Ch} \left(\frac{E}{E_{th}} \right) dE \qquad (13)$$

with the normalization

$$\int_{-\infty}^{+\infty} G_r^e(r; s, h) \, d \log r = 1 \qquad (14)$$

Of course, the LD of Ch light *emitted* by the electrons will be the same, so that

$$G_r^{Ch}(r; s, h) = G_r^e(r; s, h) \qquad (15)$$

The parametrization of the above distribution is presented in the Appendix.

The results of our calculations are shown in Fig. 3. The parametrization functions are also presented and it can be seen that the fit is everywhere better than 5%.

2.2.4 A comparison of the importance of lateral and angular distributions of electrons

To check on the influence of the two distributions (lateral and angular) on the LDCh at some level we have compared the rms radii of the ChL distribution, r_{rms}, that would have resulted from each of these distributions alone. The situation is demonstrated in Fig. 4 where such a comparison is shown. The chosen level is at $s = 1.2$ (1050 g cm^{-2}) for a typical proton shower with $E_0 = 10^{19}$ eV.

The curves show r_{rms} of the LDCh contributions produced at level X (per unit path), as would have been observed if electrons had had no lateral spread, r_θ, and if they had had no angular spread, $r_\perp$. r_θ equals the distance between the level X and that corresponding to $s = 1.2$ ($X \simeq 1050$ g cm^{-2}), multiplied by the root mean square tangent of the angle of Ch electrons at level X. These two radii show effective spreads of ChL if only one distribution (lateral or angular) had been responsible for it. If both distributions were independent from each other the resulting mean square distance would be the sum of the squares of both radii. Thus, the smaller one must be comparable to the larger, to be important. We can see that it is the contributions from only the last ~ 100 g cm^{-2} for which the lateral distribution of electrons plays a role.

10
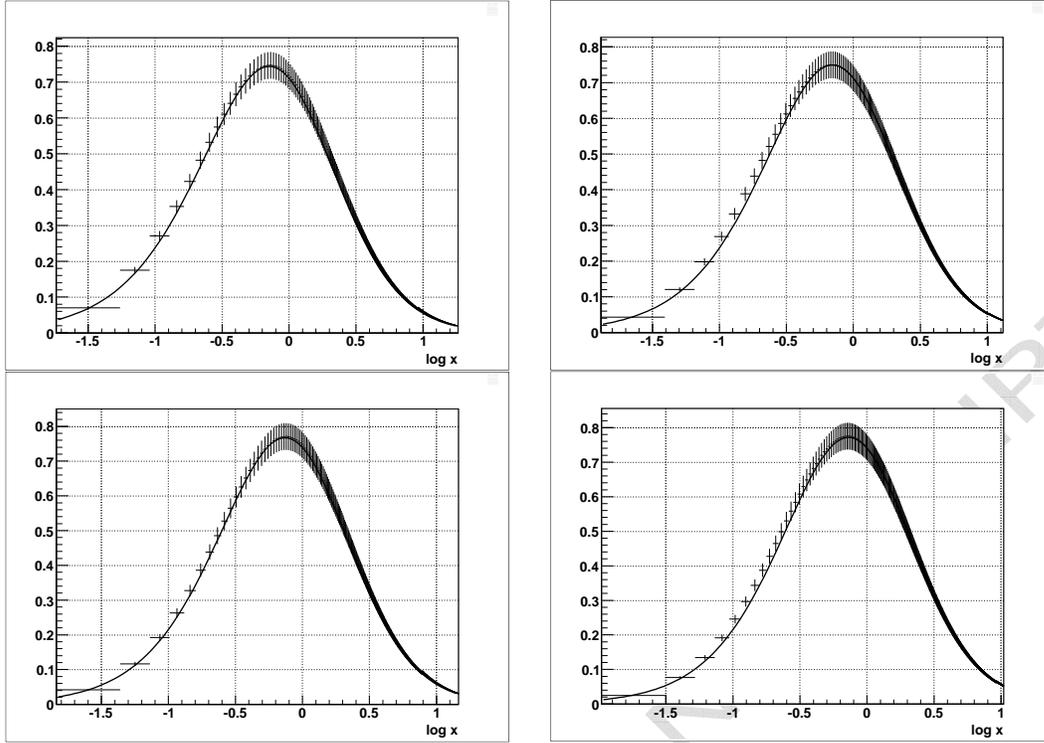
Fig. 3. Lateral distributions of Ch light, $G_r^{Ch}(r; s, h)$, emitted at $s=1$ – two upper graphs and $s=1.2$, – lower graphs, left graphs – $h=5$ km, right graphs – $h=8$ km. Points – results of calculation, lines – best fit parametrization. Error bars represent 5% of the value.
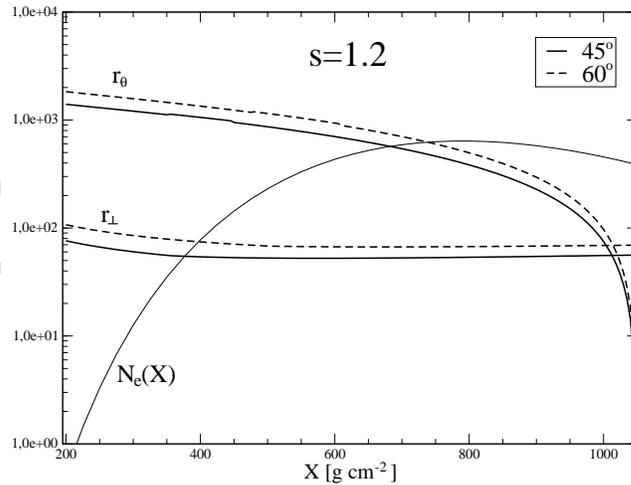
Fig. 4. Root mean square (in meters) of the lateral distribution of Ch light, produced at X and observed at depth $X_{obs} = 1050$ g cm^{-2}; r_θ – if Ch electrons had only an angular distribution (no lateral spread), $r_\perp$ – if Ch electrons had only a lateral distribution (no angular spread). Two curves for each case correspond to zenith angles z = 45°, 60°. Also shown is the shower curve $N_e(X)$ (in arbitrary units).

11

We have also ploted a curve proportional to the number of electrons $N(X)$ for a typical 10^{19} eV proton shower. It can be seen that the region of X where the lateral spread of electrons is important is rather small.

2.2.5   Final calculations of LDCh arriving at depth X_{obs}

Not withstanding the expected small influence of the LD of Ch electrons on the LDCh *arriving* at some level, we do take it into account but in a somewhat simplified way. For each slant depth element ΔX where the ChL is produced and arrives at the considered level X_{obs}, we checked which of the distributions, angular or lateral, would itself have given broader Ch lateral distribution at this level. If $r_\theta > r_\perp$ (the case for most of the shower path) then we assumed that the ChL contribution of this element has a shape following from the angular distribution of this light, but each distance r is increased by a factor $\sqrt{1 + (r_\perp/r_\theta)^2}$. Thus, the number of Ch photons, $d(\Delta N_{ch})$, produced along a shower path dX at angles $(\theta, \theta + \Delta\theta)$ equals for this case

$$d(\Delta N_{Ch}(\theta)) = k\, N_e\, F(s, h)\, G_\theta^{Ch}(\theta; s, h)\, \Delta\theta\, dX \tag{16}$$

where k is the maximum number of Ch photons produced by one electron (172 photons per g cm^{-2} in the wave band $300 - 400$ nm). These photons would have arrived at the annular element of the core distance $(r, r + \Delta r)$ at level X_{obs}, where $r = y \tan\theta$, $\Delta r = y\,\Delta\tan\theta$ and y is the distance (in length units) between the two levels X and X_{obs}. However, to allow for the lateral distribution of the emitting electrons, we assign these photons to a larger ring $(r', r' + \Delta r')$ where

$$r' = r \cdot \sqrt{1 + (r_\perp/r_\theta)^2} \qquad \text{and} \qquad \Delta r' = \Delta r \cdot \sqrt{1 + (r_\perp/r_\theta)^2} \tag{17}$$

In the opposite case, if $r_\perp > r_\theta$ then

$$d(\Delta N_{Ch}(r')) = k\, N_e\, F(s, h)\, G_r^{Ch}(r; s, h)\, \Delta \log r\, dX \tag{18}$$

where $G_r^e(r; s, h)$ is the LD of Ch electrons at (s, h), $r' = r \cdot \sqrt{1 + (r_\theta/r_\perp)^2}$ and $d(\Delta N_{ch}(r'))$ is the number of photons assigned to the annular distance element $(r', r' + \Delta r')$.

This procedure gives in any of these cases a lateral distribution of ChL for which

$$\left\langle r^2 \right\rangle = r_\theta^2 + r_\perp^2 \tag{19}$$

12

that would ensure the correct value of $\langle r^2 \rangle$ if the two distributions were independent of each other. As they are not (more distant electrons have lower energies and, what follows, larges angles) we underestimate the calculated LDCh. We think, however, that this underestimation is rather small because, as can be seen in Fig. 4, the region of X where both distributions have comparable widths (so that a correct calculation of the contribution of ChL from there to the total LDCh at level (s_{obs}, h_{obs}) would be needed) is small.

To allow for extinction, the numbers of photons in (16) and (18) need to be multiplied by a transmission factor $T \left[\frac{X_{obs} - X}{\cos \alpha} \right]$. It is enough to adopt that

$$\alpha = \arctan \left(\sqrt{\langle r^2 \rangle} / y \right) \tag{20}$$

The atmospheric transmission properties change quite considerably, so that the actual LDCh depends on the particular time the shower occured. However, we shall show results of LDCh calculations for some typical atmospheric conditions in § 3.

2.3 Dependence on zenith angle

All the above considerations apply to showers with any zenith angle, i.e. the lateral and angular distributions of ChL *produced* at a given level in the atmosphere depend only on shower age s and height h in the atmosphere, independently of the shower zenith angle z. It does not mean, of course, that the LDCh *arriving* at some level and, in consequence, the LD of the Ch light *scattered* at this level, does not depend on the shower zenith angle z.

Let us consider how the LDCh depends on z. For each vertical shower with a given energy, with a cascade curve $N(X)$, there is equally often (per unit solid angle, time and area) an inclined shower, at some zenith angle z, with the same $N(X)$. It is easy to show that its maximum will be higher in the atmosphere by

$$\Delta h = -H \cdot \ln \left[\cos(z) \right] \tag{21}$$

where H is the exponential scale height of the atmospheric density. The situation is shown in Fig. 5 where we have roughly sketched both showers and, perpendicularly to shower axes, the number of particles $N(X)$. We can obtain $N(h; z)$ for the inclined shower by shifting the vertical shower up by Δh and then projecting the number of particles horizontally on the inclined axis, so
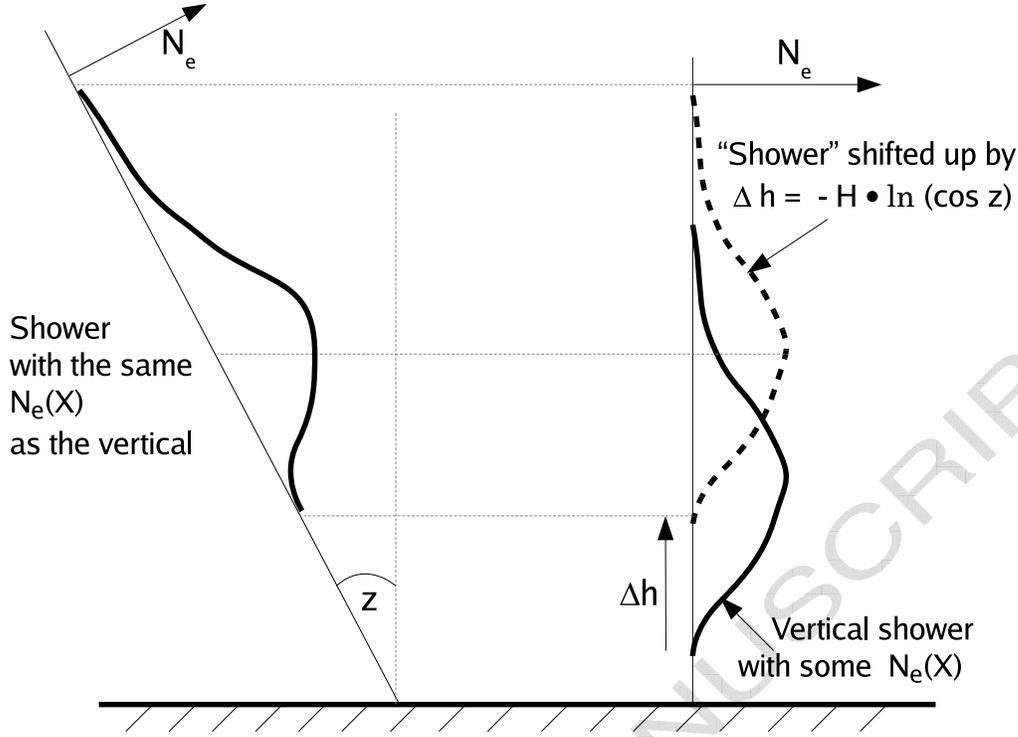
Fig. 5. Illustration of a geometrical situation of two showers having the same $N(X)$ but different zenith angles. The inclined shower can be constructed from the vertical one by shifting it by some heigth Δh and then projecting on the inclined line.

that

$$N(h; z) = N(h - \Delta h; z = 0) \tag{22}$$

The inclined shower is more elongated than the vertical one, when measured in units of length. Any shower element $dX(X)$ has a distance y to a fixed level X_{obs} (where we are calculating LDCh) larger by a factor $1/cos(z)$ than the corresponding element $dX(X)$ in the vertical shower. If all electrons had emitted ChL then the LDCh would have been the same if lateral distances were scaled by this factor. As the Molière radius (in meters) at the level higher by Δh increases also by $1/\cos(z)$, then the LDCh expressed as a function of $x = r/r_M$ would have been the same in the showers having the same $N(X)$, independent of their zenith angles.

However, the threshold energy of the element dX of the inclined shower is higher by factor $1/\sqrt{\cos(z)}$ so that there is less Ch light and the LDCh is slightly steeper. This is demonstrated in Fig. 6.

Showers, however, do fluctuate, mainly due to the fluctuations of the depth of the first interaction. Let us compare two showers, one vertical, another inclined (as before), but now with the same $N(X - X_{max})$. Assume that the inclined

14

shower initiated deeper in the atmosphere than the vertical one, so that both maxima are at the same height above the observation level. It is easy to show then that the inclined shower will be more compressed than the vertical one, in the sense that the slant distances (in length) between levels with the same $X - X_{max}$ are smaller in the inclined shower that in the vertical one. This will influence the LDCh making it narrower.

In conclusion, even if the atmosphere had been ideally stable with a known dependence $X(h)$, to calculate LDCh at some level in a shower *in advance* an additional parametrization of it as a function of zenith angle z and depth of shower maximum X_{max} would be necessary (apart from that on s and h).

3   Results of calculations of LDCh

As we have already mentioned, to calculate the LDCh at a particular level in a shower it is necessary to know the attenuation and scattering properties of the atmosphere. As these depend on the season and may change from one night to another, or even within one hour or so, constant atmosphere monitoring is needed. This is being performed e.g. in the Auger experiment [7,20]. However, to show what will be a typical width of a shower image in ChL and compare to it with that in fluorescence light, it is enough to adopt typical atmosphere properties.

Here we have assumed an atmosphere corresponding to the average conditions at the Pierre Auger Observatory in Argentina, with the mean free path for Rayleigh scattering $\lambda_R = 18.4$ km and for aerosol (Mie) scattering $\lambda_M = 14$ km at the Auger level. The exponential scale heights are correspondingly $H_R = 7.5$ km and $H_M = 1.2$ km.

In the experiments using the fluorescence technique the telescopes look at showers from the side (at rather large angles to shower directions). Thus, to compare both widths, in ChL and FL, of a shower image we have to calculate the ChL scattered sideways from the shower direction. As the FL is emitted isotropically from any shower element and the Rayleigh scattering is roughly isotropic ($\sim 1 + \cos^2 \theta$) we compare here numbers of Ch photons Rayleigh scattered in all directions. The proportion of the two components will be almost the same as if observed from any particular direction.

The results of calculations are presented in Fig. 6. We have chosen three levels of shower development: $s = 0.9$, 1.1 and 1.3 for which a comparison of the lateral spread of the scattered ChL with that of FL is shown. The curves are for typical proton and iron showers, inclined at three zenith angles: $0°$, $45°$ and $60°$. The curve representing FL does not depend on zenith angle, nor on primary
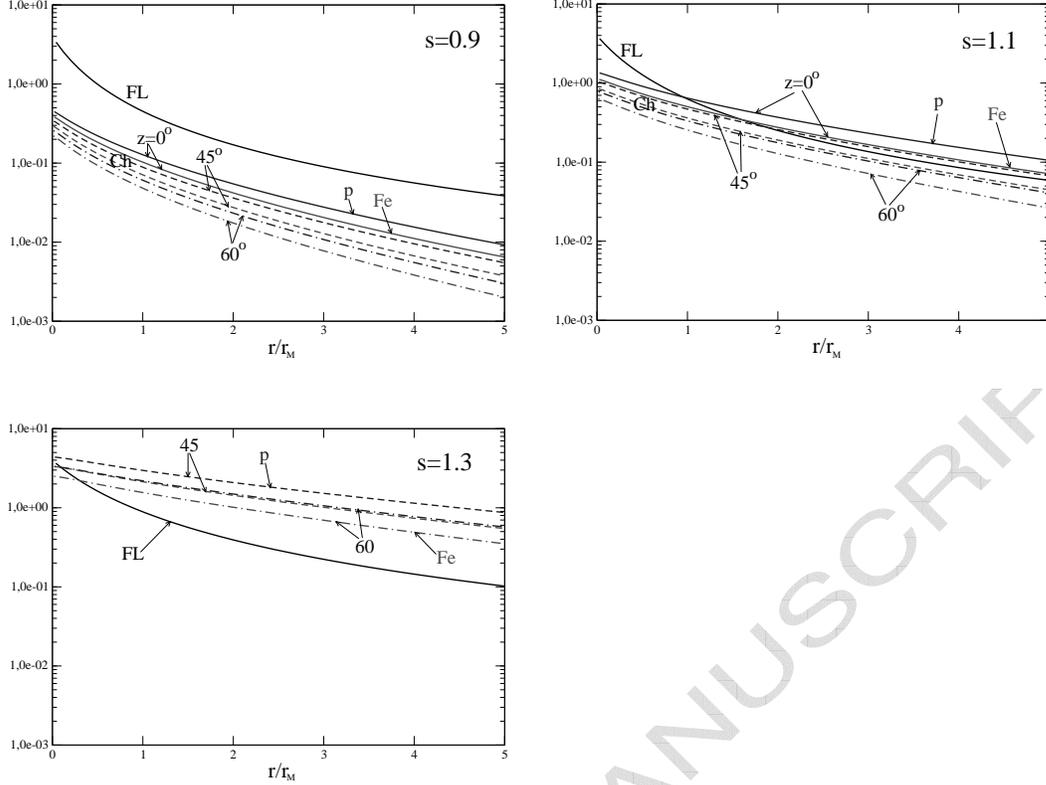
Fig. 6. Number of Ch photons scattered at distances larger than r, (per 1 m) divided by total number of electrons, N_e, compared with the fluorescence light (line marked FL) produced at distances larger than r along the same path. Three graphs correspond to values of age: s=0.8, 1.1, 1.3. Curves for proton showers are higher than those for Fe; curves for larger zenith angles are lower. The importance of ChL on the lateral width of the shower light image is evident below the shower maximum.

particle, as the lateral distribution of shower electrons depends on shower age only, if represented as a function of r/r_M (as has been discussed earlier). To calculate the FL curves we have used the parametrisation of Góra et al [12]. In calculating widths of shower images these authors take into account FL only. Our results show that this is proper only for widths above (in height) shower maximum ($s < 1$). Fig. 6 shows that at $s = 0.9$ the contribution of the ChL to the FL is small. However, when s increases the ChL contribution increases also. For $s = 1.1$ (Fig.6) it starts to dominate FL above one Molière radius, or so. Even deeper in the atmosphere ($s = 1.3$) it is the ChL which practically determines the lateral spread of the image. This corresponds to the Auger level for a 10^{19} eV proton shower with $z = 45°$. Thus, the LDCh can not be neglected when reconstructing the energy losses of shower particles at these levels, which are *proportional to the fluorescence intensity only.*

The Rayleigh (molecular) scattering is not the only process relevant. The ChL can also be scattered by aerosols present in the lower parts of the atmosphere, what is called the Mie scattering. The angular distribution of light scattered

16

by this process depends on the size of the aerosol droplets, but for any size the distribution is rather strongly peaked forward. Thus, the Mie scattered light will contribute a little to the total light from showers observed usually at rather large angles to their axes.

However, a contribution of the Mie scattered light can be easily taken into account:

Let us denote by λ_R and λ_M the mean free paths for Rayleigh and Mie scatterings respectivelly, and by $f_R(\theta)$ and $f_M(\theta)$ the angular distributions of the scattered light for the two processes. If a shower is observed at an angle θ, then the full contribution of the scattered ChL (by both processes) can be obtained by multiplying our values from Fig. 6 by

$$1 + \frac{\lambda_R f_M(\theta)}{\lambda_M f_R(\theta)} \tag{23}$$

For example, at 2 km above the Auger level (~ 1450 m) the mean free paths would be $\lambda_R = 24$ km and $\lambda_M = 74$ km, for the values given in § 3. Then the factor (23) allowing for the Mie scattering, for $f_M(\theta) = 0.8 \cdot \exp(-\theta/26.7°)$, is equal to 1.53 for $\theta = 45°$. It is strongly dependent on the height as the Mie scale height H_M is only ~ 1.2 km.

4   Discussion

A proper reconstruction of the energy losses, and in consequence, of the primary energy, depends of course on how well the shower light is recovered. The data from a FL detector are in a form of the camera PMTs response in consecutive time bins (100 ns in Auger). To recover the actual signals in the consecutive time bins one looks around the direction towards the shower at a particular time (we assume that the geometry of the shower is known) and finds the total signal in the PMTs inside a viewing cone with an opening angle ζ. Summing up signals over all time bins and finding the opening angle ζ for which the signal S to noise N ratio is the largest one can hope that the signal of the whole track is contained within the viewing cone.

However, as ζ is the same for the whole track but the track width becomes larger when going down, it may happen that the light from lower parts of a shower will be cut out by too small an angle ζ.

This angle depends on the distance to the shower. Barbosa et al [21] calculated that the optimal angle ζ for a 5 km distant shower was $\sim 2.4°$. We calculate that for a 10^{19} eV proton shower with $z = 45°$ the signal from the level $s = 1.3$

17

(just above the earth at Auger) would be collected from within $r/r_M < 2.1$ cutting out almost half of ChL and $\sim$9% of Fl. (The same would happen for a 10 km distant shower and $\zeta = 1.2°$.) If all Ch light was subtracted from the signal this would decrease the infered FL signal from this level by $\sim$40%. We estimate that the primary energy of such nearby showers could be underestimated by $\sim$15% or so.

5 Summary and conclusions

We have shown that the lateral spread of the scattered Ch light has an important role in determining the width of the optical image of a shower, particularly below shower maximum. This result has been obtained without time-consuming simulations of extremely high energy showers dedicated to Cherenkov light. To do this, we have used our earlier results showing universality of the properties of large showers. We have also derived that the angular and lateral distributions of Ch electrons at some level in the atmosphere, responsible for the width of the optical image of a shower, depend on shower age and height of this level only. Thus, the properties of the ChL produced at a particular level in the atmosphere depend only on the height h of this level and the stage of the shower development, measured by the age parameter s. It is advisable to parametrize the angular distribution of ChL at this stage, as the parametrization of the image width would have to depend on another two parameters X_{max} and z.

A full understanding of the optical shower image is nessesary to correctly infer the energy losses of shower particles along their propagation in the atmosphere. If the LDCh was broader than it is aknowledged then too much ChL could be subtracted from the total signal, leading to an underestimation of the shower primary energy.

6 Aknowledgments

7 Appendix

7.1 Parametrization of the angular distribution of the emitted Ch light, $G_\theta^{Ch}(\theta; s, h)$

Having found numerically $G_\theta^{Ch}(\theta; s, h)$ we have parametrized it (similarly as in [9] for all electrons) as follows

$$G_\theta^{Ch}(\theta; s, h) = \frac{1}{N_{Ch}} \frac{dN_{Ch}}{d\theta} = \begin{cases} a_1 \cdot e^{-(c_1 \cdot \theta + c_2 \cdot \theta^2)} & \text{for } \theta < \theta_0 \\ \\ a_2 \cdot \theta^{-\alpha} & \text{for } \theta > \theta_0 \end{cases} \tag{24}$$

Parameters of the distribution (24) are dependent on s and h (in km, above sea level) in the following way:

$$b(s, h) = p_0 \cdot e^{p_1 \cdot s + p_2 \cdot h} + p_3 \tag{25}$$

where $b = \theta_0$, a_1, c_1 and α,

and:

$$c_2(s, h) = p_0 \cdot e^{p_1 \cdot s^2 + p_2 \cdot h} + (p_3 \cdot s^2 + p_4 \cdot s) \tag{26}$$

for parameter c_2.

a_2 can be obtained from the condition of continuity of the angular distribution at θ_0.

The values of the parameters have been found by a minimization procedure, to fit best the numerical values. They are given in the table below.

p_i	θ_0	a_1	c_1	c_2	α
p_0	6.058e+00	2.905e+00	7.320e+00	-2.754e+00	2.620e+00
p_1	-1.103e-03	-3.851e-02	-3.778e-01	-4.242e-01	6.837e-02
p_2	-2.886e-03	1.072e-01	7.202e-02	1.084e-01	-2.247e-02
p_3	-5.447e+00	1.066e+01	7.143e+00	3.344e+00	1.110e+00
p_4				-4.294e+00	

The deviation of the parametrization functions from the numerically calculated values reach $\sim 10\%$ at large angles. They are, however, a few percent for small angles.

7.2   Parametrization of the lateral distribution of the emitted Ch light, $G_r^{Ch}(r; s, h)$

We have parametrized the lateral distribution $G_r^{Ch}(r; s, h)$ as follows:

$$G_r^{Ch}(r; s, h) = C \cdot \left(\frac{r}{r_M}\right)^{\alpha} \cdot \left(1 + k\frac{r}{r_M}\right)^{-\beta} \tag{27}$$

where C guarantees the correct normalisation, and equals:

$$C = \ln(10) \cdot k^{\alpha} \frac{\Gamma(\beta)}{\Gamma(\alpha)\Gamma(\beta - \alpha)} \tag{28}$$

The dependence on s and h (in km, above sea level) is as follows:

$$\alpha(s, h) = (p_0 \cdot s^3 + p_1 \cdot s + p_2 \cdot h + p_3 \cdot s \cdot h + p_4) \cdot (h + p_5) + p_6 \tag{29}$$

$$k(s, h) = e^{p_0 \cdot s^2 + p_1 \cdot h + p_2 \cdot s} \cdot (p_3 \cdot h^2 + p_4 \cdot s \cdot h + p_5 \cdot s) + p_6 \tag{30}$$

$$\beta(s, h) = e^{p_0 \cdot s^2 \cdot h + p_1 \cdot h^2 + p_2} + p_3 \cdot s + p_4 \tag{31}$$

The values of the parameters are:

p_i	α	k	β
p_0	-6.087e-04	-9.864e-01	1.206e-01
p_1	5.619e-02	1.599e-01	9.075e-03
p_2	3.428e-03	1.947e+00	-6.902e+00
p_3	-2.618e-03	7.696e-05	5.509e-01
p_4	-6.003e-02	-4.462e-03	2.757e+00
p_5	8.200e+00	6.259e-02	
p_6	1.235e+00	5.858e-01	

20

References

[1] F. Kakimoto et al., Nucl. Instrum. Methods A 372 (**1996**) 527

[2] P. Colin et al., Astropart. Phys. 27 (**2007**) 317

[3] C. Song et al., Astropart. Phys. 14 (**2000**) 7

[4] R.M. Baltrusaitis et al., Nucl. Instrum. Methods A 240 (**1985**) 410

[5] T. Abu-Zayyad et al., Astroparticle Journal 557 (**2001**) 686

[6] R.U. Abbasi et al., Astropart. Phys. 23 (**2005**) 157

[7] J. Abraham et al., Nucl. Instrum. Methods A 523 (**2004**) 50

[8] M. Giller, G. Wieczorek, A. Kacperczyk, H. Stojek, W. Tkaczyk, J. Phys. G: Nucl. Part. Phys. 30 (**2004**) 97

[9] M. Giller, A. Kacperczyk, J. Malinowski, W. Tkaczyk, G. Wieczorek, J. Phys. G: Nucl. Part. Phys. 31 (**2005**) 947

[10] F. Nerling, J. Blümer, R. Engel, M. Risse, Astropart. Phys. 24 (**2006**) 421

[11] M. Unger, B.R. Dawson, R. Engel, F. Schüssler, R. Ulrich, Nucl. Instrum. Methods A 588 (**2008**) 433

[12] D. Góra et al., Astropart. Phys. 24 (**2006**) 484

[13] B. Dawson, M. Giller, G. Wieczorek, Proc. 30th ICRC, Mérida (**2007**) 651

[14] M. Giller, H. Stojek, G. Wieczorek, Int. J. Mod. Phys. A, No. 29 (**2005**) 6821

[15] B. Rossi and K. Greisen, Rev. Mod. Phys. 13, (**1941**) 240

[16] K. Kamata J. Nishimura, Suppl. Prog. Theo. Phys. 6 (**1958**) 93

[17] A.M. Hillas, J. Phys. G: Nucl. Part. Phys. 14 (**1982**) 1475

[18] D. Heck, J. Knapp, J.N. Capdevielle, G. Schatz, T. Thouw, Report FZKA 6019 (**1998**)

[19] M. Giller, A. Kacperczyk, W. Tkaczyk, Proc. 30th ICRC, Mérida (**2007**) 632

[20] B. Keilhauer et al., Astropart. Phys. 22 (**2004**) 249

[21] H. Barbosa et al., Proc. 29th ICRC, Pune 7 (**2005**) 21